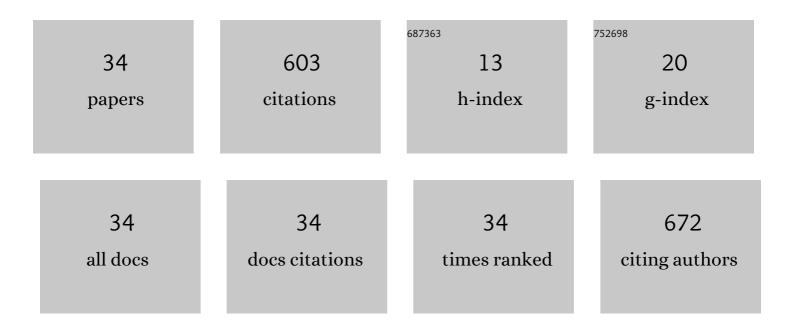


## List of Publications by Year in descending order

Source: https://exaly.com/author-pdf/6836318/publications.pdf Version: 2024-02-01



ΕΛΝΙ \λ/μ

#	Article	IF	CITATIONS
1	Rice Crop Monitoring in South China With RADARSAT-2 Quad-Polarization SAR Data. IEEE Geoscience and Remote Sensing Letters, 2011, 8, 196-200.	3.1	97
2	A Novel Hierarchical Ship Classifier for COSMO-SkyMed SAR Data. IEEE Geoscience and Remote Sensing Letters, 2014, 11, 484-488.	3.1	69
3	Earthquake-Induced Building Damage Detection with Post-Event Sub-Meter VHR TerraSAR-X Staring Spotlight Imagery. Remote Sensing, 2016, 8, 887.	4.0	63
4	Urban Building Change Detection in SAR Images Using Combined Differential Image and Residual U-Net Network. Remote Sensing, 2019, 11, 1091.	4.0	46
5	Time-Series InSAR Monitoring of Permafrost Freeze-Thaw Seasonal Displacement over Qinghai–Tibetan Plateau Using Sentinel-1 Data. Remote Sensing, 2019, 11, 1000.	4.0	45
6	Built-up area mapping in China from GF-3 SAR imagery based on the framework of deep learning. Remote Sensing of Environment, 2021, 262, 112515.	11.0	31
7	Multitemporal Water Extraction of Dongting Lake and Poyang Lake Based on an Automatic Water Extraction and Dynamic Monitoring Framework. Remote Sensing, 2021, 13, 865.	4.0	26
8	Investigation of the Capability of \$Hhbox{-}alpha\$ Decomposition of Compact Polarimetric SAR. IEEE Geoscience and Remote Sensing Letters, 2014, 11, 868-872.	3.1	24
9	Capability of Rice Mapping Using Hybrid Polarimetric SAR Data. IEEE Journal of Selected Topics in Applied Earth Observations and Remote Sensing, 2015, 8, 3812-3822.	4.9	24
10	Paddy Rice Mapping in Thailand Using Time-Series Sentinel-1 Data and Deep Learning Model. Remote Sensing, 2021, 13, 3994.	4.0	24
11	Signature Analysis of Building Damage With TerraSAR-X New Staring SpotLight Mode Data. IEEE Geoscience and Remote Sensing Letters, 2016, 13, 1696-1700.	3.1	23
12	Classification of Vessels in Single-Pol COSMO-SkyMed Images Based on Statistical and Structural Features. Remote Sensing, 2015, 7, 5511-5533.	4.0	20
13	MW-ACGAN: Generating Multiscale High-Resolution SAR Images for Ship Detection. Sensors, 2020, 20, 6673.	3.8	20
14	SAR Image Super-Resolution Based on Noise-Free Generative Adversarial Network. , 2019, , .		14
15	Automatic Detection of Low-Rise Gable-Roof Building from Single Submeter SAR Images Based on Local Multilevel Segmentation. Remote Sensing, 2017, 9, 263.	4.0	10
16	Spaceborne SAR Data for Regional Urban Mapping Using a Robust Building Extractor. Remote Sensing, 2020, 12, 2791.	4.0	10
17	Permafrost Soil Moisture Monitoring Using Multi-Temporal TerraSAR-X Data in Beiluhe of Northern Tibet, China. Remote Sensing, 2018, 10, 1577.	4.0	9
18	Polarimetric synthetic aperture radar change detection for specific land cover types. International Journal of Digital Earth, 2015, 8, 334-344.	3.9	8

Fan Wu

#	Article	IF	CITATIONS
19	An adaptive two-scale enhancement method to visualize man-made objects in very high resolution SAR images. Remote Sensing Letters, 2015, 6, 725-734.	1.4	7
20	Detectability Analysis of Road Vehicles in Radarsat-2 Fully Polarimetric SAR Images for Traffic Monitoring. Sensors, 2017, 17, 298.	3.8	6
21	Soil Moisture Estimation based on the Distributed Scatterers Adaptive Filter over the QTP Permafrost Region using Sentinel-1 and High-resolution TerraSAR-X Data. International Journal of Remote Sensing, 2021, 42, 902-928.	2.9	6
22	An Anchor-Free Method for Arbitrary-Oriented Ship Detection in SAR Images. , 2021, , .		5
23	Discrimination of Collapsed Buildings from Remote Sensing Imagery Using Deep Neural Networks. , 2019, , .		4
24	High-voltage transmission towers detection using hybrid polarimetric SAR data. , 2014, , .		3
25	The estimation of the absolute phase of polarimetric wave changed by the target. , 2015, , .		2
26	Earthquake-Induced Building Damage Assessment on SAR Multi-Texture Feature Fusion. , 2020, , .		2
27	Damage building analysis in TerraSAR-X new staring spotlight mode SAR imagery. , 2015, , .		1
28	Geometrical characteristics based building height extraction from VHR SAR imagery. , 2017, , .		1
29	Ship detection and velocity estimation in quad polarimetric SAR images from pursuit monostatic mode of TerraSAR-X and TanDEM-X. , 2017, , .		1
30	Corn Fine Classification With Gf-3 High-Resolution Sar Data Based on Deep Learning. , 2019, , .		1
31	Automatic Extraction of Built-Up Areas for Cities in China from GF-3 Images Based on Improved Residual U-Net Network. , 2020, , .		1
32	Building features extraction based on facade regularities using TerraSAR-X ST data. , 2015, , .		0
33	Building classification from single TerraSAR-X ST image by fusing structure features in the pyramid framework. , 2017, , .		0
34	Permafrost Subsidence Monitoring of Qinghai-Tibet Plateau using Sentinel-1 Data. , 2019, , .		0